Pure Appl. Geophys. 172 (2015), 921–929

DOI 10.1007/s00024-014-0936-2

Pure and Applied Geophysics

Development of a Tsunami Inundation Map in Detecting Tsunami Risk in Gulf of Fethiye, Turkey

Derya Itir Dilmen,[1] Serkan Kemec,[2] Ahmet Cevdet Yalciner,[3] Sebnem Düzgün,[4] and Andrey Zaytsev[5]

Abstract—NAMIDANCE tsunami simulation and visualization tool is used to create tsunami inundation maps showing quantitative maximum tsunami flow depths in Fethiye. The risk of an extreme, but likely earthquake-generated tsunami is estimated at Fethiye Bay for 14 probabilistic earthquake scenarios. The bay is located 36°39′5″N 29°7′23″E, southwestern Turkey, which has coastline to the eastern Mediterranean Sea. The tsunami simulation and inundation assessment are performed in three stages: (1) formation of a digital elevation model of the region from the best available topography/bathymetry dataset, (2) estimation of a maximum credible tsunami scenario for the region and determination of related earthquake parameters, (3) high resolution tsunami simulation and computation of near shore and overland tsunami dynamics in the study area using tsunami simulation and visualization code NAMIDANCE, (4) determination of spatial distributions of tsunami characteristics (maximum water elevations, water velocities, flow depths) under the critical tsunami condition. The results are based on the most recent descriptions of potential tsunami sources, topographic and bathymetric databases, and tsunami numerical models. We present an innovative study concentrating on preparation of quantitative flow depths and inundation maps with a very high-resolution bathymetry/topographic dataset in the eastern Mediterranean. Inundation maps will be used to analyze the effects of possible tsunamis. The presented research is crucial to raising the awareness of government officials, the public, and other stake holders about the high probability of a tsunami event in Turkey. Moreover, the results of this study will help to plan for evacuation routes, establish safe zones, and assist in preparation for the tsunami, creating public awareness, and planning evacuation routes before the actual tsunami event happens.

Key words: Tsunami, Fethiye, NAMIDANCE, Inundation map, Mediterranean.

1. Introduction

The Eastern Mediterranean Basin has encountered numerous tsunamis even though they have a low frequency of occurrence in comparison to the Pacific and Indian Oceans. Historical documents and geological field investigations reveal that tsunamis occurred due to high seismicity, volcanic eruptions, and submarine/sub aerial landslides in the eastern Mediterranean region in the last 3,500 years. These events have been documented by many scholars.[1] Cita and Rimoldi (1997), Yalciner *et al.* (2007a), and Papadopoulos (2009) found evidence of tsunami deposits in Fethiye Bay as a result of geological investigations. Altinok *et al.* (2011) presents the most recent tsunami catalogue which contains 134 previously recorded tsunamis between the years 1410 BC and 2000. Forty-two of these tsunamis caused loss of property and damage in the Fethiye. In Minoura *et al.* (2000), the tsunami deposits found in Fethiye Calis beach (North of Sovalye Island) related to the 1630 BC Santorini event have been documented. Historical accounts of events and geological investigations warn that

[1] Earth and Space Sciences Department, University of Washington, Seattle, USA. E-mail: dilmen@uw.edu
[2] Department of City and Regional Planning, Yüzüncü Yıl University, Van, Turkey. E-mail: skemec@yyu.edu.tr
[3] Department of Civil Engineering, Middle East Technical Universit, Ankara, Turkey. E-mail: yalciner@metu.edu.tr
[4] Department of Mining Engineering, Middle East Technical University, Ankara, Turkey. E-mail: duzgun@metu.edu.tr
[5] Special Research Bureau for Automation of Marine Researches, Far Eastern Branch of Russian Academy of Sciences, Moscow, Russia. E-mail: aizaytsev@mail.ru

[1] Galanopoulos (1960), Ambraseys (1962), Antonopoulos (1979), Papadopoulos and Chalkis (1984), Soloviev (1990), Papazachos (1990), Amiran *et al.* (1994), Cita and Rimoldi (1997), Tinti and Maramai (1996), Cita *et al.* (1996), Guidoboni and Comastri (1997), Soloviev *et al.* (2000), McCoy and Heiken (2000), Minoura *et al.* (2000), Rebesco *et al.* (2000), Altinok *et al.* (2001), Dawson *et al.* (2003), Salamon *et al.* (2007) and Yolsal *et al.* (2007).

Birkhäuser

waves would be more damaging today due to increased coastal population and utilization in the area. Therefore, detailed assessment of the probable tsunami risk based on very high-resolution topographic and bathymetric datasets and reliable tsunami sources are necessary to be prepared for the next probable tsunami.

Numerical studies (Dilmen, 2009 and Yalciner *et al.,* 2011) to estimate the maximum inundation limit in Fethiye and surrounding bays were conducted. These studies indicate that tsunami waves reach run-up values up to 3 m at the northern coast of Fethiye Bay. These results do not take into account the detailed risk assessment of the coastal infrastructures due to the limited resolution (15 m) of bathymetric/topographic datasets for the region.

In the present study, a high resolution bathymetry and coastal topography dataset (3 m) collected for Fethiye is used to determine the tsunami risk estimated from 14 tsunami scenarios at the Gulf of Fethiye. We use a numerical model of tsunami generation, propagation, and inundation (NAMIDANCE) to investigate and estimate the effects of a range of probable tsunami sources on the coast of Fethiye. The goals of the present research are to analyse the probable tsunami risk at Fethiye Bay and to develop tsunami inundation maps showing flow depths quantitatively.

The remainder of the paper is organized as follows: Sect. 2 introduces study area. Section 3 describes tsunami numerical model and simulations. Discussion and conclusions are presented in Sect. 4.

2. Study Area

Fethiye is a city and district of the Mugla Province of Turkey situated in the eastern part of the Mediterranean Basin (see Fig. 1). Fethiye and the surrounding region consist of a very narrow shelf and a large canyon connecting the deep bottom of Rhodes Basin with Fethiye Bay. The shelf is wider along the inner margins of the Fethiye and Marmaris Bays. The shelf's maximum depth is 350 m (Ocakoglu 2012). This area is highly prone to earthquakes, volcanic activities and submarine landslides due to its proximity to active plate boundary zone between the Eurasian and African Plates that could be an initiative source of a probable tsunami.

3. Tsunami Numerical Model and Simulations

The tsunami numerical simulation and visualization code NAMIDANCE is used to compute the tsunami parameters of extreme, but probable tsunamis. The model computes tsunami wave generation, propagation, and inundation by solving non-linear, shallow-water wave Eqs. (1–3). These equations are solved numerically using the finite difference technique and leap-frog scheme for basins of irregular shape and bathymetry with four layers of telescoping grids (Goto and Ogawa 1991; Yalciner *et al.* 2006; Imamura *et al.* 1989). The smallest grid has the highest resolution.

$$\frac{\partial \eta}{\partial t} + \frac{\partial M}{\partial x} + \frac{\partial N}{\partial y} = 0 \tag{1}$$

$$\frac{\partial M}{\partial t} + \frac{\partial \eta}{\partial x}\left(\frac{M^2}{D}\right) + \frac{\partial}{\partial y}\left(\frac{MN}{D}\right) + gD\frac{\partial \eta}{\partial x} + \frac{k}{2gD^2}M\sqrt{(M^2+N^2)} = 0 \tag{2}$$

$$\frac{\partial N}{\partial t} + \frac{\partial \eta}{\partial y}\left(\frac{N^2}{D}\right) + \frac{\partial}{\partial x}\left(\frac{MN}{D}\right) + gD\frac{\partial \eta}{\partial y} + \frac{k}{2gD^2}N\sqrt{(M^2+N^2)} = 0 \tag{3}$$

Here, η is water surface elevation, M and N are discharge fluxes in the x and y directions, respectively, D is total water depth, H is the undisturbed basin depth, and k is the bottom friction coefficient.

The model has been extensively tested against the analytical and experimental benchmark problems (Briggs et al. 1995; Kanoglu 2004; Kanoglu *et al.* 2013) and verified by field data of the 2004 Indian Ocean tsunami event and 2011 Great East Japan Earthquake and Tsunami (Okal and Synolakis 2004; Yalciner *et al.* 2007a, b, Yalciner *et al.* 2011). The model is successfully applied to historical tsunami simulations such as 1867 Virgin Islands (Zahibo *et al.* 2003), 1883 Krakatau (Choi *et al.* 2003), 2004 Indian Ocean (Choi *et al.* 2005; Yalciner *et al.* 2006), and tsunami scenarios in the Mediterranean (Yalciner

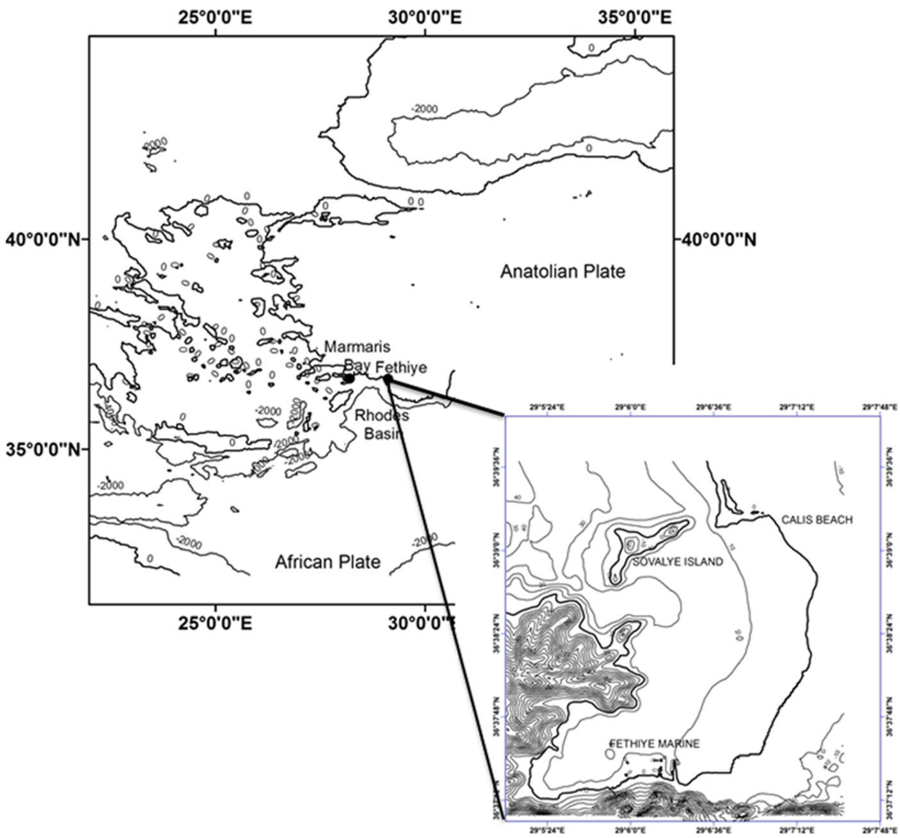

Figure 1

Plate boundaries of the study region are given as contour maps (*left inset*). Location of Fethiye Bay, Fethiye Marine, and Calis Beach are depicted at the *right inset*

et al. 2002, 2004) and Caribbean Seas (Kurkin *et al.* 2003).

3.1. Tsunami Model Set-Up

Maximum tsunami wave amplitudes and flow depths are computed to estimate the extreme, but plausible tsunami risk and to create inundation maps of the Fethiye Bay. The simulation described hereafter is initialized with a highly accurate bathymetry/topography and a worst-case tsunami source. The model setup of four layers of nested B, C, D, and E grids are created from 3 m resolution of topography/bathymetry of Fethiye (see Fig. 2). Table 1 includes the list of nested grid boundaries. The resolution of the innermost grid for the simulations presented in this study is 3 m (1/10 s). Manning's roughness coefficient is taken as $n = 0.025$. The simulation takes 5 h in real time.

3.1.1 Bathymetry/Topography Dataset

Bathymetric and topographic datasets for the Gulf of Fethiye are obtained by numerous methods in different terrestrial environments and at various scales and resolutions (see Table 2). It expresses geomorphologic features and the shoreline detailed enough so that it takes into account of the local effects for accurate tsunami propagation and run-up results.

The coordinates and elevation of Fethiye shoreline are measured with differential GPS. It has the horizontal and vertical accuracy of 20 cm. A highly accurate digital elevation model at near-shore bathymetry and topography is generated with high-resolution Airborne Quickbird Multispectral Satellite Imagery. General Bathymetric Chart of the Oceans (GEBCO) data of 180 m (1 min) resolution is used for the location and elevation data of the offshore region. All data are assessed for quality and accuracy within each dataset to

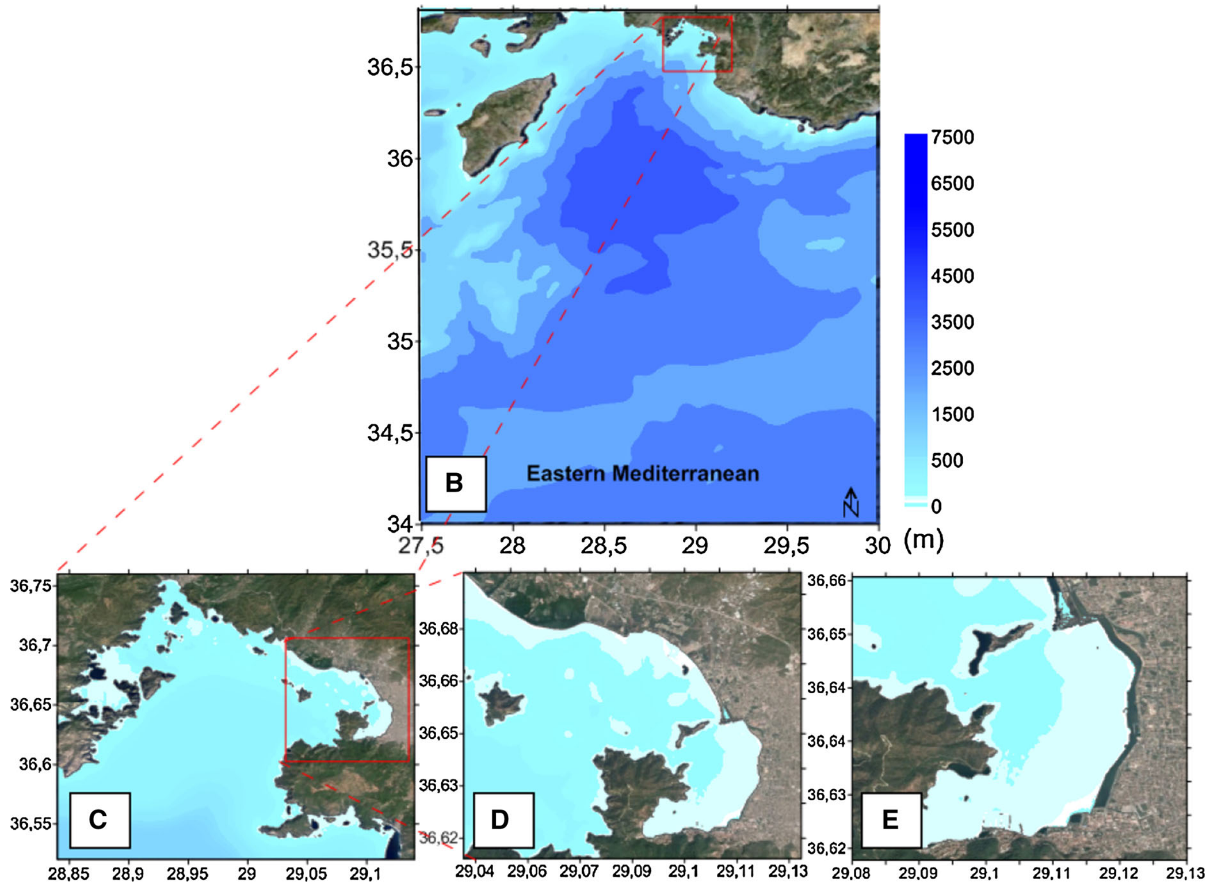

Figure 2
Nested B–C–D–E grids are overlaid with Google Earth Image. The innermost grid E has the highest resolution of 3 m (1/10 s)

ensure consistency of the data and gradual topographic transitions along the edges. The final created DEM's horizontal datum is World Geodetic System 1984 (WGS-1984) and vertical datum is taken as mean sea level due to the maximum tide difference of 30 cm.

3.1.2 Tsunami Source Estimation

Fourteen extreme, but likely sea floor deformations between 7.5 and 8.4 (Table 3) are initialized to be the worst case tsunami source scenarios based on the deliverables of Tsunami Risk and Strategies for the European Region (TRANSFER) Project partners.[2] Parameters of these scenarios are given in Table 3. These parameters are used to estimate probabilistically the tsunami risk at Fethiye Bay. Return periods for the earthquake sources are estimated as 500 and 1,000 years by FORTH(2). METU-OERC(2) and NOAGI(2) follow a deterministic approach for initial source estimation. According to seafloor deformation results, METU-OERC(2) earthquake source 10 generates highest uplift and subsidence of initial tsunami source and highest maximum wave amplitudes inside the harbor at selected virtual synthetic gauges. The

Table 1

NAMIDANCE model grid boundary coverage and cell size for Fethiye

Grids	Longitude (°N)	Latitude (°E)	Cell size (m)
B	27.5–30	34–36.8	300
C	28.84–29.14	36.52–36.76	100
D	29.04–29.13	36.61–36.69	33
E	29.08–29.13	36.62–36.68	3

[2] Foundation for Research and Technology Hellas (FORTH), National Observatory of Athens Institute of Geodynamics (NOAGI), and Middle East Technical University Ocean Engineering Research Center (METU-OERC).

Table 2

Detailed information of collected bathymetric and topographic data

Name	Date	Method	Projection (GCS)	Vertical accuracy (m)	Horizontal accuracy (m)
Quickbird multispectral image	1994	Erdas imagine	WGS-1984	2.44	3.66
Coastline data	2007	GPS	WGS-1984	0.2	0.2
Bathymetric data	2007	Field measurements	WGS 1984	3.7	5
Bathymetric data	2007	GEBCO	WGS 1984	10	180

Table 3

Probable Tsunami source parameters

	Longitude (°N)	Latitude (°E)	Dip (°)	Rake (°)	Strike (°)	Depth (m)	*M*w	*L* (km)	*W* (km)	Slip (m)
500 year occurrence probability tsunami source by FORTH										
1	28.462	36.447	27	99	294	7.5	7.71	86	43	2.49
2	28.434	36.077	47	262	184	7.5	7.53	70	35	2.00
3	28.393	35.821	25	90	303	7.5	7.45	64	32	1.85
1,000 year occurrence probability tsunami source by FORTH										
4	28.462	36.447	27	99	294	7.5	8.04	126	63	3.65
5	28.434	36.077	47	262	184	7.5	7.84	100	50	2.90
6	28.393	35.821	25	90	303	7.5	7.76	91	45	2.70
FORTH worst case scenarios										
7	28.400	35.500	20	90	55	7.5	8.35	190	90	5.00
8	28.400	35.500	20	90	55	10.0	8.12	140	70	4.00
9	29.000	36.200	20	90	300	7.5	8.01	150	35	5.00
METU-OERC										
10	29.000	36.660	10	110	210	50.0	8.16	175	60	6.00
11	27.780	34.200	45	45	60	40.0	7.96	136	40	6.00
12	28.480	35.160	45	45	60	40.0	7.93	122	40	6.00
NOAGI estimated source parameters										
13	28.200	36.000	20	90	135	20.0	7.50	86	25	2.00
14	28.500	36.350	20	90	285	20.0	7.50	86	25	2.00

uplift and subsidence map of this source is given in Fig. 3.

3.2. Simulations

Tsunami simulation of Fethiye Bay is performed with and without inclusion of Sovalye Island to the bathymetric and topographic datasets. Virtual gauges are placed to compare synthetic tsunami waveforms for the worst-case tsunami scenario at the entrance of the bay and inside the bay. The time histories of virtual gauges Offshore 01 and D-1 are shown and plotted at Fig. 4. In the simulations while the wave motion and possible amplifications inside Fethiye Bay are evaluated, the wave attenuation effect of the Sovalye Island in front of the bay was also examined by performing additional simulation with the absence of Sovalye Island. The time histories of water surface elevations at two virtual gauge points outside the bay (Offshore-1) and inside the bay (D-1) are plotted in Fig. 4 with or without Sovalye Island cases.

Time histories of the selected gauges show that tsunami waves arrive to Fethiye Bay at less than 10 min. The waves reach 2.1 m elevation inside the bay at numerical gauge point D-1. The maximum water elevation at numerical gauge point D-1 increases to 2.6 m at the case where Sovalye Island is not included at the bathymetry (see Fig. 4).

3.3. Tsunami Inundation Map for the Worst-Case Scenario: 10

A map of quantified tsunami maximum flow depths and inundation results overlaid with Google

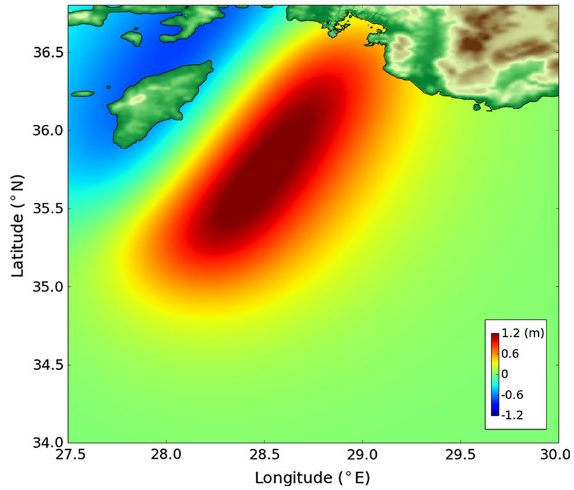

Figure 3
METU-OERC tsunami scenario 10. *Red* and *blue colors* represent the uplift and subsidence of scenario 10, respectively

Earth Image for Fethiye Bay are shown in Fig. 5. Computed tsunami flow depths and inundation are shown on the map in three color-coded depth ranges: 0–0.5, 0.5–2, and >2 m. These depth ranges are chosen because they are approximately knee-high or less, knee-high to head-high, and more than head-high to represent the degree of hazard for life safety. The greatest tsunami flooding is expected to occur on low lands close to Calis Beach on the northeastern shores of Fethiye Bay.

Elsewhere, tsunami flooding occurs in areas of low topography at the shoreline that have maximum flow depths exceeding 3 m due to the existing conditions. The protection level of Sovalye Island has been investigated by performing simulations with and without the existence of the island. We assert that Sovalye Island, located at the entrance of the bay, partly reduces the impact of the tsunami inside the bay.

4. Discussion and Conclusions

We present the spatial distribution of maximum tsunami flow depths and inundation areas as a result of the tsunami model for the extreme, but plausible tsunami. There was uncertainty regarding the likely earthquake epicenter and the fault rupture mechanism that could cause the worst-case tsunami scenario. Therefore, 14 probable earthquakes were selected, and the rupture parameters of these earthquakes were chosen from project deliverables of the EU funded

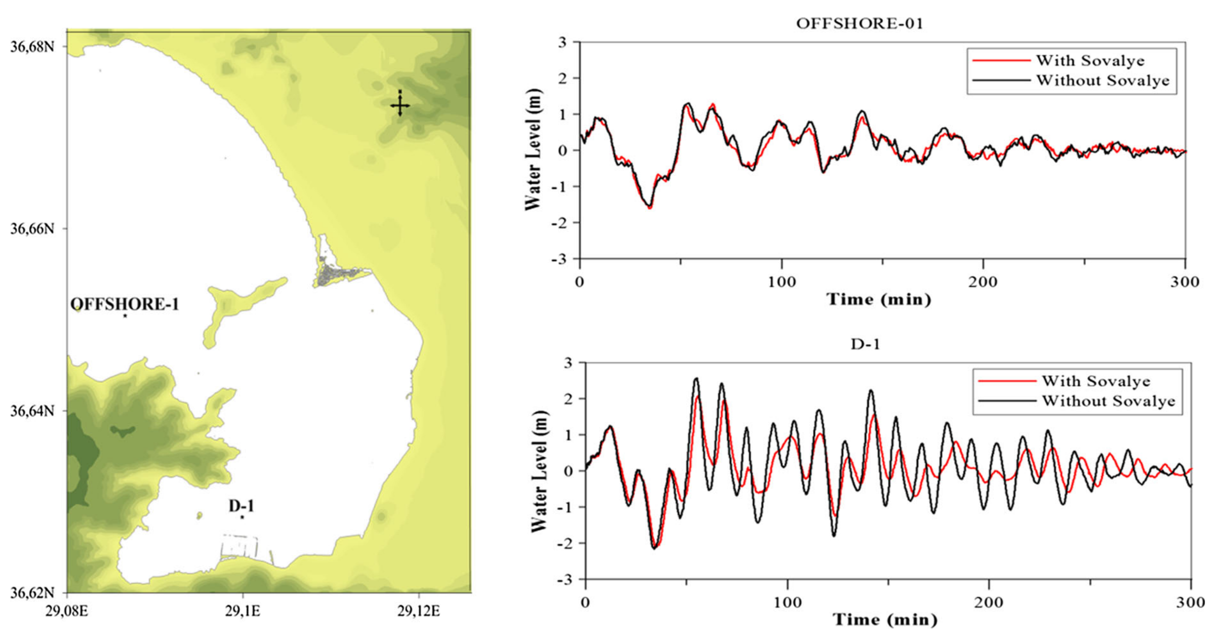

Figure 4
Location of the selected virtual gauges (*left inset*) and modeled water levels (m) at the virtual gauges of OFFSHORE-01 (40 m depth) and D-1 (10 m depth) for scenario 10 (*right inset*)

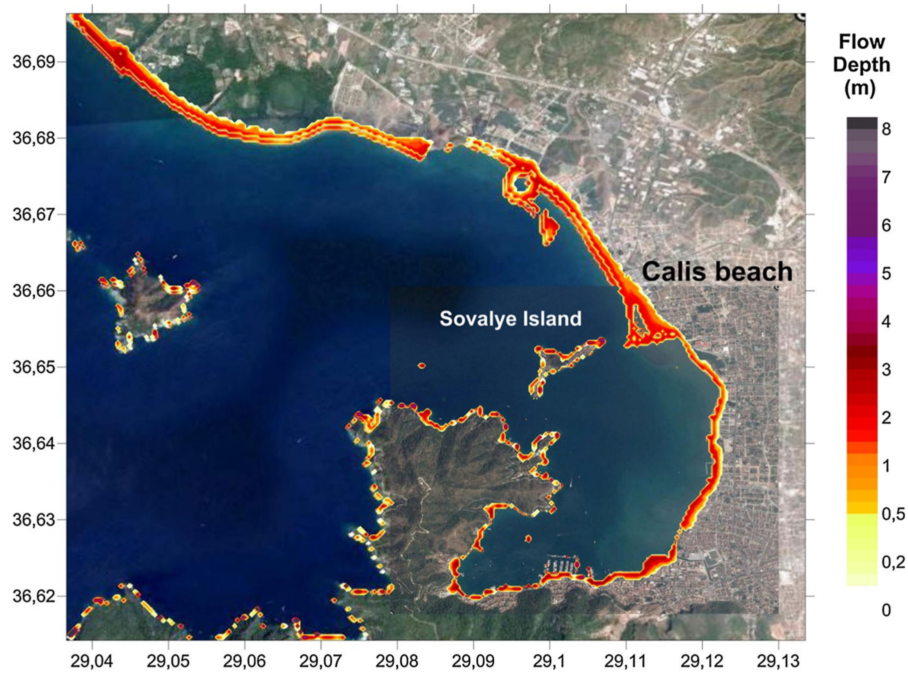

Figure 5
Tsunami inundation map shows the maximum flow depths due to maximum probable tsunami source METU-OERC 10 in Fethiye Bay

research, Tsunami Risk and Strategies for European Union (TRANSFER), as potential sources of earthquakes and tsunamis. The earthquake that gives the highest amplitudes in front of Fethiye bay and maximum tsunami flow depths on the Fethiye coast was selected as worst-case tsunami scenario. Simulation of worst-case scenario gave us the quantitative map of inundated areas showing, maximum possible tsunami flow depths, and inundation boundaries.

Inundation is higher in shallow and low-land nearshore regions with flat onshore topography, like the northeastern part of Fethiye Bay. Other areas along the lowland also displayed significant flow depths of more than 3 m, thus showing that in the case of a tsunami, significant inundation is likely to occur. These areas correspond to high-density populated areas including recreational facilities and other infrastructure such as housing, hotels, parks, and restaurants. The existence of these structures in regions with flat topography increases the potential damage of a tsunami.

Sovalye Island located in front of the Fethiye Bay partly prevents entering the tsunami energy inside the bay. On the other hand, it prevents the outgoing of the tsunami energy and causes long duration agitation inside the inner bay. Therefore, the coastal amplification and inundation inside the bay remain significant. The sandy beach at the north coast outside the bay will receive the direct impact of tsunami waves, and hence more inundation distances and flow depths will be observed there.

Tsunami flow depths and inundation limits presented here are computed without the inclusion of the bottom friction due to infrastructures on land. This fact might result in slight overestimation of inundation and flow depths. In spite of this limitation, the results presented here allow the identification of the most vulnerable areas quantitatively that should be evacuated in case of a tsunami in the region.

Incorporation of the information generated from the numerical models provided to determine the areas that could be potentially affected by tsunamis affords policy makers an additional level of preparedness. Because of increasing population and city development throughout the northeastern coasts of Fethiye Bay, it is necessary to disseminate the results to inform locals of the level of threat in their region. The dissemination of this information will provide an additional level of confidence for visitors and residents of coastal locales. Therefore, our research can serve as a guideline for the development of quantitative tsunami risk maps for the eastern Mediterranean region.

Acknowledgments

This study is partly supported by TRANSFER and SEAHELLARC Projects granted by European Commission, UDAP-Ç-12-14 project granted by Disaster Emergency Management Presidency of Turkey (AFAD), and 108Y227 project by TUBITAK and DPT 2011K140210 Projects.

References

Altinok Y., Ersoy S., Yalciner A. C., Alpar B. and Kuran U. (2001), Historical Tsunamis in the Sea of Marmara. International Tsunami Symposium, Session 4, pp. 4–2.

Altinok Y., Alpar B. Ozer N, Aykurt H. (2011), *Revision of Tsunami Catalogue Affecting Turkish Coasts and Surrounding Regions*, Natural Hazards Earth Syst. Sci., *11*, pp. 273–291.

Ambraseys N. N, (1962), *Data for the Investigation of Seismic Sea Waves in the Eastern Mediterranean*, Bull., Seism., Soc., Am., *52*, pp. 895–913.

Amiran, D.H.K., Arieh, E. & Turcotte, T. (1994), Earthquakes in Israel and Adjacent Areas: Macroseismic Observations since 100 B.C.E., *Israel Exploration Journal*, *44*, 260–305.

Antonopoulos, J. (1979) Catalogue of tsunamis in the eastern Mediterranean from antiquity to present times. Annali Di Geofisica, Vol. *32*, p. 113–130.

Briggs M., Synolakis C., Harkins G., Green D. (1995), *Laboratory Experiments of Tsunami Run-up on Circular Island*., Pure and Applied Geophysics, *144* (3/4), pp. 569–563.

B. H. Choi, E. Pelinovsky, K.O. Kim, and J.S. Lee (2003), *Simulation of the Trans-oceanic Tsunami Propagation due to the 1883 Krakatau Volcanic Eruption*, Natural Hazards and Earth Sciences, *3*, pp. 321–332.

Choi, Hong, Hwang., Hidayat, Kaistrenko, Korolev, Kurkin, Pelinovsky,Yalciner, (2005), Catastrophic tsunami in the Indian Ocean (December 26, 2004): data of two field surveys and numerical simulation. Sumatra Tsunami on 26 December 2004, Conference on Sumatra Tsunami on Dec. 26, 2004, Special Asia Tsunami Session, 2, pp. 159–188.

Cita M. B., Camerlenghi A. and RImoldi B., (1996), Deep-sea Tsunami Deposits in the Eastern Mediterraneasn: New Evidence and Depositional Models, Sediment. Geol. *104*, 155–173.

Cita M. B., Rimoldi. B. (1997), *Geological and Geophysical Evidence for a Holocene Tsunami Deposit in the Eastern Mediterranean Deep-Sea Record*, Journal of Geodynamics, *24* (1), pp. 293–304. doi:10.1016/S0264-3707(96)00030-0.

Dawson A. G., Lockett P., Shi S., (2003), *Tsunami Hazards in Europe*, Environmental International, *30*, pp. 577–585.

Dilmen, (2009), GIS Based Tsunami Inundation Maps: Case Studies from Mediterranean, Master Thesis, Middle East Technical University.

Galanopoulos A., (1960), *Tsunamis Observed on the Coasts of Greece from Antiquity to Present Time*. Annali di Geofisica, *13*, pp. 369–386.

Goto, C. and Ogawa, Y., (1991), Numerical Method of Tsunami Simulation With the Leap-Frog Scheme, Translated for the TIME Project by Prof. Shuto, N., Disaster Control Res. Cent., Faculty of Eng., Tohoku Univ. Sendai, Japan.

Guidoboni E. and Comastri A., (1997). The large Earthquake of 8 August 1303 in Crete: Seismic Scenario and Tsunami in the Mediterranean Area. Journal of Seismology, *1*, 55–72

Imamura F., (1989), Tsunami Numerical Simulation with the Staggered Leap-frog Scheme, School of Civil Engineering, Asian Inst. Tech. and Disaster Control Research Center, Tohoku University.

Kânoglu, U. (2004): *Nonlinear evolution and runup-rundown of long waves over a sloping beach*. J. Fluid Mech., 513, 363–372.

Kânoglu, U., Titov. V., Aydın B., Moore C., Stefanakis S. T., Zhou H., Spillane M., Synolakis C. E., (2013): *Focusing of long waves with finite crest over constant depth* Proc. R. Soc. A. 2013 469 2153 20130015; doi:10.1098/rspa.2013.0015 (published 27 February 2013) 1471–2946.

Kurkin A.A., Kozelkov A.C., Zaitsev A.I., Zahibo N., and Yalciner A., (2003), *Tsunami risk for the Caribbean Sea Coast. Izvestiya*, Russian Academy of Engineering Sciences, *4*, pp. 126–149.

MaramaiS., A. and Graziani, L., (2004), *The New Catalogue of Italian Tsunamis*, Natural Hazards, Vol. *33*, No. 3, pp. 439–465.

McCoy, F. W. and Heiken, G., (2000), Tsunami Generated by the Late Bronze Age Eruption of Thera (Santorini), Greece, Pure and Applied Geophysics, v.*157*:1227–1256.

Minoura K., Imamura F., Kuran U., Nakamura T., Papadopolous G., Takahashi T., Yalciner A. C., (2000), *Discovery of Minoan Tsunami Deposits*, Geology, V. *28*, No. 1, pp. 59–62.

Ocakoglu, (2012), *Investigation of Fethiye-Marmaris Bay (SW Anatolia): seismic and morphologic evidences from the missing link between the Pliny Trench and the Fethiye-Burdur Fault Zone*, Geomarine Letters, *32*:17–28 doi:10.1007/s00367-011-0234-2.

Okal E. and Synolakis (2004), Source discriminants for near-field tsunamis, Geophys. J. Int. *158*, 899–912, doi:10.1111/j.1365-246X.2004.02347.X

Papadopoulos G. A., (2009) Tsunamis. In: the Physical Geography of Mediterranean, by J.C. Woodward (ed.), Oxford Univ. Press, Oxford, p.493–512.

Papadopoulos G. A. and Chalkis, B. J., (1984), *Tsunamis observed in Greece and the surrounding area from antiquity to the present times*, Marine Geol. *56*, pp. 309–317 (footnote 1).

Papazachos B. C. (1990), Seismicity of the Aegean and Surrounding Area, Tectonophysics, *178*, 27–308

Rebesco M. B., Vedova B., Cernobori L., Aloisi A. (2000), *Acoustic Facies of Halocene Megaturbidites in the Eastern Mediterranean*, Sediment. Geol., *135*, 65–74.

Salamon A., Rockwell T., Ward S. N., Guidoboni E., and Comastri A., (2007), *Tsunami Hazard Evaluation of the Eastern Mediterranean: Historical Analysis and Selected Modeling*, Bulletin of Seismological Society of America, *97*, 705–724.

Soloviev, S., Solovieva O. N, Chan N. G., Khen S. K., Shcetnikov N. A. (2000), *Tsunamis in the Mediterranean Sea: 2000 B.C.*

- *2000 A.D.* Translation from Russian to English by Gil B. Pontecorvo and Vasiiy I- Tropin; Kluwer Academic Publishers, Dordrecht, The Netherlands, 2000, 237.

SOLOVIEV, S.L. (1990), Tsunamigenic Zones in the Mediterranean Sea. Natural Hazards, Vol. *3*, 1990, pp 183–202.

TINTI S. and MARAMAI, A. (1996), *Catalogue of Tsunamis Generated in Italy and in Côte d' Azur, France: A Step towards a Unified Catalogue of Tsunamis in Europe*, Annali di Geofisica, *39*, pp. 1253–1299.

YALCINER A. C. ALPAR B., ALTINOK Y., OZBAY I., IMAMURA F., (2002), *Tsunamis in the Sea of Marmara: Historical Documents for the Past, Models for Future* Marine Geology, 2002, *190*, pp. 445–463.

YALCINER, A., PELINOVSKY, E., TALIPOVA, T., KURKIN, A., KOZELKOV, A. and ZAITSEV, A., (2004), *Tsunamis in the Black Sea: Comparison of the Historical, Instrumental, and Numerical Data*, J. Geophys. Res., AGU, V *109*, C12023, doi:10.1029/2003JC002113.

YALCINER, A.C., KARAKUS, H. and KURAN, U (2006), Modeling of Tsunamis in the Eastern Mediterranean and Comparison with Caribbean, Caribbean Tsunami Hazard, World Scientific, ISBN: 981-256-535-3, 326–340.

YALCINER, A. C., PELINOVSKY, E., ZAITSEV, A., KURKIN, A., OZER, C., and KARAKUS, H., (2007a), Modeling and visualization of tsunamis: Mediterranean examples, from, Tsunami and Nonlinear Waves (Ed: Anjan Kundu), Springer, 2007, pp. 2731–2839.

YALCINER A., PELINOVSKY E., ZAYTSEV A., OZER C., KURKIN A., KARAKUS H., OZYURT G., (2007b), Modeling and visualization of tsunamis: Mediterranean examples, in book: Tsunami and Nonlinear Waves Kundu Anjan, Springer, pp. 273–283.

YALCINER A. C., SUPPASRI A., MAS E., KALLIGERIS N., NECMIOGLU O., IMAMURA F., OZER C., ZAYTSEV A., OZEL M. N., SYNOLAKIS C., (2011), *Field Survey on the Coastal Impacts of March 11, 2011 Great East Japan Tsunami*, Submitted to Journal of Pure and Applied Geophysics, (in review).

YOLSAL, S., TAYMAZ, T. and YALCINER, A.C., (2007), Understanding tsunamis, potential source regions and tsunami-prone mechanisms in the Eastern Mediterranean Geological Society, London, Special Publications, *291*, pp. 201–230.

ZAHIBO, N., PELINOVSKY, E., YALCINER, A., KURKIN, A., KOSELKOV, A., and ZAITSEV, A. (2003), *The 1867 Virgin Island Tsunami: Observations and Modelling*. Oceanologica Acta, *26*, pp. 609–621.

(Received April 29, 2014, revised September 15, 2014, accepted September 18, 2014, Published online October 25, 2014)